Food Chemistry 228 (2017) 167–176

Contents lists available at ScienceDirect

Food Chemistry

journal homepage: www.elsevier.com/locate/foodchem

Influence of microwave vacuum drying on glass transition temperature, gelatinization temperature, physical and chemical qualities of lotus seeds

Yingting Zhao [a], Yajun Jiang [a], Baodong Zheng [a,b], Weijing Zhuang [a,b], Yafeng Zheng [a,b], Yuting Tian [a,b,*]

[a] College of Food Science, Fujian Agriculture and Forestry University, Fuzhou, Fujian 350002, PR China
[b] Fujian Provincial Key Lab of Quality Science and Processing Technology in Special Starch, Fuzhou, Fujian 350002, PR China

ARTICLE INFO

Article history:
Received 17 October 2016
Received in revised form 25 January 2017
Accepted 28 January 2017
Available online 1 February 2017

Keywords:
Amino acid
Color
DSC
Microwave vacuum drying
Rehydration capacity
Starch
Water state

ABSTRACT

This study investigated the effects of microwave power density on effective moisture diffusion coefficient (D_{eff}), glass transition temperature (T_g), gelatinization temperature (T_P), physical and chemical qualities of lotus seeds during microwave vacuum drying. D_{eff} increased by 42% and 127% at 15 W/g and 20 W/g, respectively, when compared with 10 W/g. T_P was negatively correlated with the relaxation times of T_{21} and T_{22}, while T_g was negatively correlated with the relative areas A_{22}. The rates of change of color were observed to be divided roughly into two periods, consisting of a rapid change caused by enzymatic browning and a slow change caused by non-enzymatic browning. An equation is provided to illustrate the relationship of k_1 and k_2 of Peleg's model depending on power density during rehydration kinetics. The samples at 20 W/g exhibited the higher content of amino acid (540.19 mg/100 g d.b.) while lower starch (17.53 g/100 g d.b.).

© 2017 Elsevier Ltd. All rights reserved.

1. Introduction

Lotus (*Nelumbo nucifera* Gaertn.) is renowned as a highly sought-after functional food, and is cultivated extensively in Fujian, Hunan, Jiangxi, and Zhejiang provinces in China (Wu et al., 2007). As a traditional Chinese herbal medicine, lotus seeds are claimed to fight tissue inflammation, resist cancer, detoxify the spleen, nourish the blood, ease the symptoms of diarrhea, and to reinforce the kidneys (Zhao, Wang, Zheng, Miao, & Tian, 2016). Despite of the outstanding health benefits, lotus seeds are rarely sold fresh, because fresh seeds have a short shelf life caused mainly by enzymatic browning, and the development of microorganisms and quality decay. Lotus seeds are commonly dried to increase their shelf life. However, traditional air dried lotus seeds are associated with unfavorable physical and chemical changes during drying period; our previous studies demonstrated the potential of using microwave vacuum drying (MVD) to produce high-quality dried lotus seeds (Tian et al., 2012). We also found microwave power density has a significant effect on drying time and physical characteristics of dried lotus seeds, such as color and rehydration ratio compared with other drying parameters during MVD (Chen, 2010). The knowledge of the heat and mass transfer mechanism such as effective moisture diffusion coefficient (D_{eff}) which is related drying parameters, is required for ideal dryer design and for producing high quality dried product (Aral & Beşe, 2016). As a result, the effect of microwave power density on D_{eff} was studied here.

One of the most important modifications in the present study is an analysis of the glass transition temperature (T_g), because the glass transition temperature of various amorphous food materials plays an important role in the processing of foods and the stability of products during storage; this occurs because at temperatures below the T_g, the diffusion-controlled deterioration in product quality is arrested or is not significant within a practical time scale (Xin, Zhang, & Adhikari, 2013). Therefore, decreasing the moisture content of food by elevating T_g provides a good method for improving the preservation of food. Xu, Li, and Yu (2014) reported that the T_g of far-infrared dried carrots increased by 40.99 °C with the moisture content decreased by 0.30 g/g d.b. In addition, MVD is a potential method that can be used to increase the T_g of lotus seeds during dehydration. Water, including not only the moisture content mentioned above but also the water state, is one of important indices that can affect seed quality during MVD. So, Time Domain Nuclear Magnetic Resonance (TD-NMR) spectroscopy was used to observe

* Corresponding author at: College of Food Science, Fujian Agriculture and Forestry University, Fuzhou, Fujian 350002, PR China.
E-mail address: etingtian@hotmail.com (Y. Tian).

http://dx.doi.org/10.1016/j.foodchem.2017.01.141
0308-8146/© 2017 Elsevier Ltd. All rights reserved.

the mobility water and low molecular weight solutes inside dried samples. Starch aging is based on starch gelatinization and affected taste. Lewandowicz, Jankowski, and Fornal (2000) observed that microwave irradiation of cereal starches at a limited moisture content (<35%) caused an increase in the starch pasting temperature; in addition, the extent of the changes was greater when the moisture content of the microwave-treated starch increased. Therefore, MVD is a potential method that could be used to increase the peak temperature (T_P) in order to decrease starch gelatinization, thus decreasing aging and preserving the original taste of lotus seeds after MVD. Importantly, only a few studies have reported on the relationship between the water state and T_g (Xin et al., 2013; Xu et al., 2014); however, few scientific studies have investigated the relationship between water state and T_g as well as T_P simultaneously.

Food products are sensitive to drying conditions. Tian et al. (2012) reported that the use of MVD to dry lotus seeds may cause some negative changes in their physical properties such as color because color was affected by many reactions during drying, including enzymatic (Schulze, Hubbermann, & Schwarz, 2014) and non-enzymatic browning (Aral & Beşe, 2016). These two kinds of browning existed simultaneously during MVD. The zero- and first-order kinetic models, which might only fit one kind of browning, did not fit the process very well when applied to MVD. Therefore, a new model needs to be selected to describe the color change of lotus seeds during MVD. Buyers of primarily use color when selecting lotus seeds and dried lotus seeds with a high rehydration ratio are also preferred by consumers. Drying conditions can also influence water migration during rehydration (Zielinska & Markowski, 2016). The Peleg model has been widely applied to describe the rehydration capacity of dried products (Peleg, 1988; Moreira, Chenlo, Chaguri, & Fernandes, 2008). Peleg's parameters were usually represented by the kinetic rate constant k_1 and the characteristic constant of Peleg's model, k_2. However, the relationship between both k_1 and k_2 with microwave power density has not been clear during rehydration periods for lotus seeds dehydrated by MVD. Besides the physical qualities, the chemical composition of final product might be changed during MVD, especially the amino acid and starch content. This was because they involved in the Maillard reaction that affects changes of color, which occurred between amino and carbonyl groups. Among the types of starch in lotus seed, lotus seed resistant starch is a type of retrograded starch that is commonly known as resistant starch type 3. This type of starch been used to prevent gastrointestinal diseases and cardiovascular disease (Zeng et al., 2015). Thereby, the chemical composition of the final product was studied under MVD.

Accordingly, the objective of this work was to initially investigate the effects of microwave power density on reducing the drying time of lotus seeds during MVD by D_{eff}. The influence of microwave power density on water state and on both T_g and T_P was examined simultaneously. Additional goals were to determine the physical and chemical qualities of dried lotus seeds, including color, rehydration capacity and chemical composition under different MVD conditions.

2. Materials and methods

2.1. Materials

Frozen fresh lotus (*Nelumbo nucifera* Gaertn.) seeds, with the fruit coat, seed coat, spire, and embryo root (*plumula nelumbinis*) removed, were obtained from Fujian Minjiang Source Lutian Industrial Investment Development Co., Ltd., Fujian, China. All samples were thawed in a 4 ± 0.5 °C water bath for 8 h prior to drying experiment. The mean initial moisture content was 1.65 ± 0.01 (g/g d.b.). The longitudinal–transverse diameter ratio of the samples (1.10) was measured according to Zheng's method (Zheng, 2004). All samples used for drying were taken from a single batch of thawed seeds.

2.2. Microwave vacuum drying

This study employed a multifunctional and programmable microwave vacuum dryer, which was designed by ourselves and manufactured by Guangzhou Kailing Industrial Microwave Equipment, Ltd. (Guangzhou, Guangdong, China). It had a maximum nominal power of 4.2 kW (Fig. S1) (Song, Zheng, & Zeng, 2009). Samples (about 200 g each) were placed uniformly in single thin layers on six plates, then put in the microwave cavity and rotated at 1 rpm during the drying processing. The microwave power density (10 W/g, 15 W/g and 20 W/g) was set experimentally using a variety of settings that are used to describe the drying characteristics of lotus seeds. A probe thermometer (Model 11025, Delta Trak Inc., Pleasanton, CA, USA) was placed into the center of lotus seeds to rapidly test the temperature of samples during drying (Chen, 2010). The drying process continued until the moisture content of lotus seed samples fell below 0.15 (g/g d.b.).

2.3. Effective moisture diffusion coefficient (D_{eff})

Moisture content and drying rate of lotus seeds were measured according to the methods of Zhao et al. (2016). The drying rate of foods normally decreases over time, because moisture loss and vapor migration are driven by diffusion. Since the various mechanisms are not separable, D_{eff} is used to describe all possible mechanisms of moisture movement and can be estimated by Fick's second law of diffusion using Eq. (1) as symbolized by a mass-diffusion equation (Pei et al., 2014):

$$MR = \frac{M - M_e}{M_0 - M_e} = \frac{8}{\pi^2}\sum_{n=0}^{\infty}\frac{1}{(2n+1)^2}\cdot\exp\left(-\frac{(2n-1)^2\pi^2\cdot D_{eff}\cdot t}{4L^2}\right) \quad (1)$$

where MR, M_0, M_e, D_{eff}, t and L are the moisture ratio, the initial moisture content (g/g d.b.), the equilibrium moisture content (g/g d.b.), effective moisture diffusivity (m^2/s), drying time (s), and sample thickness (m), which equals the distance in the radial direction from the seed center to surface, respectively, and n is a positive integer.

2.4. Differential scanning calorimeter (DSC)

The thermal properties of the lotus seed samples were measured by a differential scanning calorimeter (Pyris Diamond; Perkin-El-mer, Boston, MA, USA). In this study, samples (3.0 mg) from each treatment were encapsulated into aluminum DSC pans and 10 μL distilled water was added. The pan was hermetically sealed, equilibrated for 1 h at room temperature, and heated from 20 to 200 °C in the DSC at 10 °C/min. An empty stainless steel pan was used as reference; every measurement was performed in triplicate. The TA universal analysis software (TA Instrument Co., New Castle, DE, USA) provided with the DSC instrument was employed to assess the onset (T_{g0}), mid-point (T_g) and end (T_{ge}) of the glass transition temperature, as well as the onset (T_0), peak (T_P) and conclusion (T_c) of the gelatinization temperature.

The Gordon–Taylor model is considered to be a reliable predictor of the T_g as a function of moisture content due to its plasticizing effect. The Gordon–Taylor empirical equation is:

$$T_g = \frac{X_s(T_{gs}) + kX_w(T_{gw})}{X_s + kX_w} \quad (2)$$

where X_s and X_w (g/g total) are the corresponding mass fraction of solid matrix and water, respectively; T_g, T_{gs} and T_{gw} are the glass transition temperature of the samples, solid matrix and water, respectively; and k is the Gordon–Taylor parameter. The T_g, X_s and X_w were detected in the present study, and the T_{gw} was −135 °C. The k and T_{gs} were estimated with non-linear regression analysis using Matlab R2013a (MathWorks Inc., Natick, MA, USA).

2.5. Nuclear magnetic resonance (NMR)

NMR relaxation measurements followed methods similar to Zhao et al. (2016) using a low-field pulsed NMR 20-Analyst (MesoMR60, Shanghai Niumag Electric Corp., Shanghai, China). Carr-Purcell-Meiboom-Gill (CPMG) sequences were employed on an ^{1}H NMR spectrometer to measure the spin–spin relaxation time, T_2. These transverse relaxation spectra were obtained from CPMG decay curves, which were composed by echo intensity.

2.6. Color measurements

The color of the dried lotus seed were analyzed by measuring the reflectance using a Chroma Meter (Chroma Meter WSC-S, Shanghai Precision and Scientific Instrument Co., Shanghai, China). The Hunter Lab color system was used, where L^* represents the lightness of luminance component, and parameters a^* and b^* (from green to red and from blue to yellow, respectively) represent the two chromatic components. The ΔE was determined using Eq. (3):

$$\Delta E = \sqrt{(L_0 - L^*)^2 + (a_0 - a^*)^2 + (b_0 - b^*)^2} \quad (3)$$

where "0" refers to the color reading of fresh samples, which were used as a control. The larger ΔE, the greater color changes from the reference color.

It was assumed that each parameter follows new kinetic model which is given by Eq. (4):

$$\frac{Y - Y_e}{Y_0 - Y_e} = Aexp(kt) + ct + d \quad (4)$$

where Y is the color parameter (L^*, a^*, b^*, ΔE); Y_0 and Y_e are the corresponding initial and equilibrium values, respectively; A is related to shape of the biomass spread; k is the reaction rate constant of each color parameter; c *is* related to the relative magnitude of the parameter; d is dimensionless color kinetic constant; t is the drying time (min) (Nannyonga, Bakalis, Andrews, & Gkatzionis, 2016).

2.7. Determination of polyphenol oxidase (PPO) activities

Extraction of PPO and measurement of its activity were based on PPO kits (Nanjing Jiancheng Bioengineering Institute, Nanjing, China).

2.8. Rehydration kinetics

The rehydration ratio of the dried samples was determined by first immersing the samples into hot water at 60 °C for 30 min; then the samples were drained over a mesh for 30 ± 10 s and quickly and gently blotted by tissues 4 ± 5 times and then reweighed. The rehydration ratio is useful for determining how the dried product will react in the future when contacting moisture. A higher rehydration ratio indicates a higher recovery of the original structure in the final product. The rehydration capacity of each sample was calculated using Eq. (5):

$$\text{Rehydration ratio}(\%) = \frac{W_t - W_0}{W_t} \times 100\% \quad (5)$$

where W_t is the weight of material at any immersion time t and W_0 is the weight of the material before immersion.

In this study, the Peleg model was used for rehydration modelling. The model proposed by Peleg (1988) is as follows:

$$X_t = X_0 \pm \frac{t}{k_1 + k_2 \cdot t} \quad (6)$$

where X_0 is the initial water content expressed as dry basis (g/g d.b.) and X_t is the water content at time t (min). k_1 is the Peleg rate constant (min (g/g d.b.) $^{-1}$) and is related to the mass transfer rate at the very beginning ($t = t_0$). k_2 is the Peleg capacity constant ((g/g d.b.)$^{-1}$) and is related to maximum water absorption capacity.

$$X_e = X_0 \pm \frac{1}{k_2} \quad (7)$$

In Eq. (7) "±" becomes either "–" if the samples dehydrate or "+" if samples rehydrate. X_e is the water content when samples reach the equilibrium ((g/g d.b.)$^{-1}$) at $t \to \infty$.

In addition, the relationship between both k_1 and k_2 with microwave power density were represented with exponential Eqs. (8) and (9):

$$K_1 = k_0 \exp(-AW_p) \quad (8)$$

$$K_2 = h_0 \exp(-BW_p) \quad (9)$$

where k_1 and k_2 are obtained using Peleg's model (s (g d.b./g)), k_0 and h_0 are both pre-exponential constants (s (g d.b./g)), A and B are the constants of the model (g/W), and W_p is the microwave power density (W/g).

2.9. Chemical qualities

The ash, fat, crude protein and carbohydrate were prepared and their contents were measured using the previous method reported by Zheng (2004).

The free amino acid compositions of the samples were analyzed using an L-8900 amino acid analyzer (Hitachi, Katsuda, Japan) using procedures described in our previous study, Pei et al. (2014), with some modifications. The finely ground samples (0.25 g) were added to 10 mL 75% ethanol and then heated in a 60 °C water bath for 30 min. Then 1 ml hydrolysate was centrifuged at 10,000 rpm for 15 min and the collected supernatant was evaporated by nitrogen blowing at 50 °C. The residue was dissolved in 4 mL deionized water and diluted with 8 mL lithium citrate solution to reach a final pH value between 2 and 3. Then, the protein was removed by adding 3 mL of 3% trichloroacetic acid solution and allowed to keep at 4 °C for 1 h prior to centrifugation for 15 min at 10,000 rpm. After that, the supernatant was collected and passed through a 0.22 μm membrane filter. Twenty microlitres of the filtrate were injected using an auto-sampler for analysis. Mixed standard amino acids with taurine standard were analyzed before sampling. The amino acids in the samples were identified and quantified by comparing peak profiles of the samples with the standard profiles. The results were expressed as the milligrams of amino acid per 100 g (mg/g d.b.).

Starch, including native and amylose, in the lotus seeds was extracted and determined their content as described by Chen (2015). The resistant starch type 3 was prepared and the content of this type of starch was measured using the previously reported method of Zeng et al. (2015).

2.10. Statistical analysis

Treatments were conducted in triplicate. The experimental results obtained were expressed as means ± SD. Statistical analysis was performed using SPSS software (version 19.0, SPSS Inc., Chicago, IL, USA). All results were analyzed by analysis of variance ($p < 0.05$) and the means identified using Duncan's multiple range test. The drying experiment data were fitted to Page model using Origin 8.5 Analysis software (Giri & Prasad, 2007).

3. Results and discussion

3.1. Drying characteristics and effective moisture diffusion coefficient (D_{eff})

Fig. 1(a) shows the experimental drying curves of lotus seeds when drying was carried out using MVD at three microwave power densities: 10, 15 and 20 W/g at 20 kPa of absolute pressure. As the microwave power density increased, the moisture ratio for the same MVD time decreased. The time required for 10 W/g treated lotus seeds to reach a moisture content of 0.15 (g/g d.b.) was up to 23 min. A reduction of the drying time of 30.43% and 56.52% was observed at 15 W/g and 20 W/g, respectively. Moreover, two falling rate periods were observed in each case. Initially, the moisture content decreased more rapidly and then it decreased rather slowly until reaching equilibrium for moisture content. This occurred because moisture gradients within the samples differed in two falling rate periods. The Page model ($MR = \exp(-bt^n)$) was used to fit the curves in Fig. 1(a). The values of drying constant b reflected the rate at which water from the foodstuff was removed and b ranged from 0.081 to 0.155 at 10 W/g and 20 W/g. The increase in b can be attributed to the fact that higher microwave power density helps to enhance the reaction temperature and increase the driving force of heat and mass transfer (Giri & Prasad, 2007). This result was consistent with the reports by Evin (2012) where the k of microwave vacuum dried *Agaricus bisporus* slices ranged from 0.0098 to 0.2943 under the microwave power range of 90–180 W, respectively.

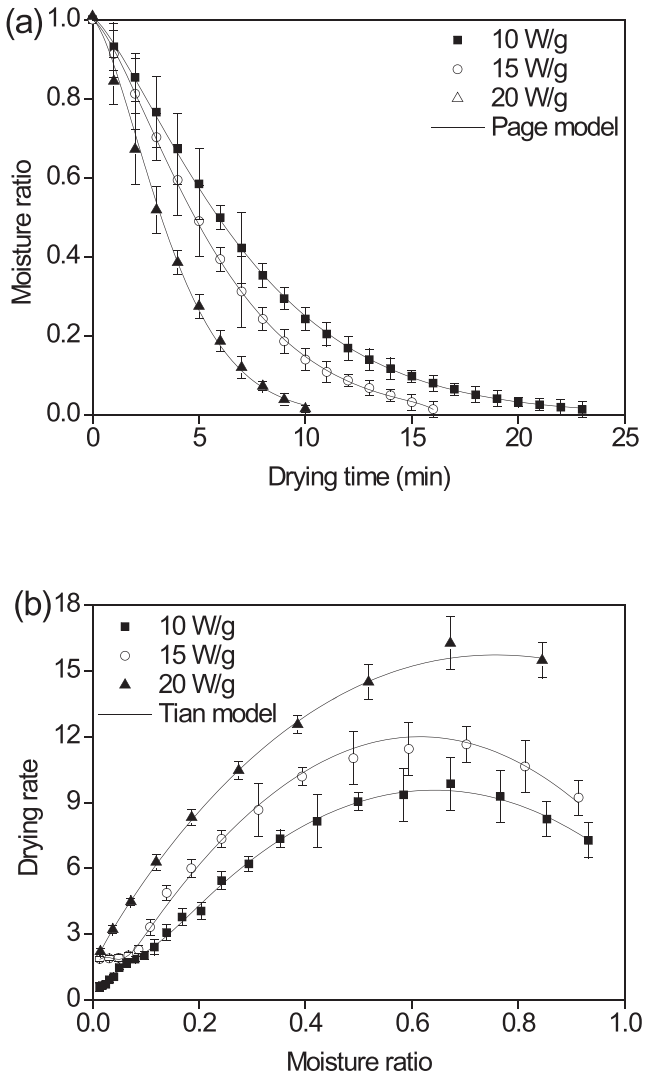


Fig. 1. Effect of microwave power density on drying curves for lotus seeds during microwave vacuum drying at 20 kPa of absolute pressure: (a) Moisture ratio vs. drying time, and Page model (Giri and Prasad, 2007) fitted to the data; (b) Drying rate vs. moisture ratio, and Tian model (Zhao et al., 2016) fitted to the data. Mean ± SD of three independent experiments.

Fig. 1(b) shows the variations of drying rate against the moisture ratio under various microwave power densities. The drying rate exhibited a unique convex shape that was observed in which the initial drying rate increased slightly followed by a decreased drying rate. The initial rate of increase could be attributed to the high microwave energy absorption when a significant amount of dipole molecules were present. The drying rate then decreased because of the internal resistance to both heat and mass transfer (Zielinska & Michalska, 2016). Furthermore, a higher microwave power density resulted in a more remarkably accelerated drying rate, because high microwave power density could increase the value of the effective moisture diffusivity (D_{eff}) (Table S1). Because rising microwave power densities result in increased heating energy which increases the kinetic energy of water molecules, moisture diffusivity increased. For example, the D_{eff} values increased by 42% and 127% at 15 W/g and 20 W/g, respectively, when compared with 10 W/g. That is, increasing microwave power density resulted in an increase in vapor pressure in the samples which causes moisture inside the samples to move faster to the surface, so the D_{eff} values increase.

3.2. DSC and NMR in microwave vacuum dried lotus seeds

3.2.1. T_g and T_P as measured by DSC

In samples with a high moisture content ($X_{ws} \geqslant 1.5$ (g/g d.b.)), T_g values were independent of the moisture content and remained constant or decreased slightly, while they increased obviously with a decreasing content of immobilized water during drying of samples having a low moisture content. This fact suggests that in samples with high moisture content, the cells of the samples represent a dilute solution system with low viscosity. In this system, the effect of the viscosity of cellular solutions is quite small. However, at a low moisture content, one cause of the elevation in the T_g with decreased moisture content is the plasticization effect of water on the amorphous constituents of the matrix (Ruiz-Cabrera, Rivera-Bautista, Grajales-Lagunes, González-García, & Schmidt, 2016). In addition, the Gordon-Taylor model is a reliable predictor of the T_g as a function of moisture content. In this study, the Gordon-Taylor model was fitted well by the experimental data at low solid mass fractions (below 0.84 (g/g d.b.)) with the following parameters: $T_{gs} = 65.55$ °C and $k = 0.06$ ($R^2 = 0.993$). The reason for this could be that no significant effect of sugar composition was observed for the k values at high solid mass fractions, while k values were significantly extrapolated from low solid mass fractions (Ruiz-Cabrera & Schmidt, 2015). The change of T_g was more significant with an increase in microwave power density (Table 1). With a decreasing moisture content to the final moisture approximately 0.15 (g/g d.b.), the values of T_g increased to 68.75, 69.82, and

Table 1
Glass transition and gelatinization characteristics of microwave vacuum dried lotus seeds.

Time (min)	Glass transition				Gelatinization characteristics			
	T_{g0} (°C)	T_g (°C)	T_{ge} (°C)	ΔC_p (J/g)	T_0 (°C)	T_P (°C)	T_c (°C)	ΔH (J/g)
Control	− 13.32 ± 0.7^{g}	− 8.49 ± 1.5^{g}	− 3.77 ± 0.3^{g}		73.73 ± 2.2^{b}	77.65 ± 2.3^{b}	81.86 ± 2.8^{e}	1.798 ± 0.071^{j}
10 W/g								
4	− 14.58 ± 0.2^{g}	− 9.52 ± 0.1^{g}	− 4.18 ± 0.9^{g}		75.77 ± 1.2^{a}	79.70 ± 1.8^{a}	83.90 ± 0.5^{de}	1.851 ± 0.042^{j}
8	19.35 ± 1.4^{f}	24.34 ± 1.8^{f}	29.32 ± 1.6^{f}		76.20 ± 1.7^{a}	80.18 ± 1.3^{a}	84.31 ± 1.4 c^{d}	2.230 ± 0.013^{i}
12	40.83 ± 0.3^{d}	45.29 ± 0.9^{d}	50.53 ± 0.1^{d}		76.58 ± 0.3^{a}	80.51 ± 0.5^{a}	84.70 ± 1.6^{bcd}	2.537 ± 0.024^{h}
16	54.25 ± 1.5^{c}	58.74 ± 1.2^{c}	64.96 ± 0.8^{c}		76.91 ± 0.4^{a}	80.83 ± 1.1^{a}	85.03 ± 0.7^{bcd}	2.784 ± 0.031^{f}
20	62.44 ± 0.1^{b}	67.23 ± 0.3^{b}	72.31 ± 1.2^{b}		77.18 ± 1.5^{a}	81.09 ± 0.6^{a}	85.39 ± 0.8^{abcd}	2.959 ± 0.042^{e}
23	68.75 ± 0.2^{a}	73.94 ± 0.8^{a}	78.47 ± 1.5^{a}	0.082 ± 0.005^{a}	77.43 ± 0.9^{a}	81.31 ± 1.2^{a}	85.56 ± 1.6^{abcd}	3.028 ± 0.018^{d}
15 W/g								
3	− 14.44 ± 0.6^{g}	− 9.39 ± 0.3^{g}	− 4.07 ± 0.5^{g}		75.83 ± 2.1^{a}	79.89 ± 0.3^{a}	83.99 ± 1.5^{de}	1.842 ± 0.074^{j}
6	21.13 ± 2.1^{ef}	26.15 ± 1.6^{f}	31.95 ± 0.3^{e}		76.29 ± 0.6^{a}	80.31 ± 1.2^{a}	84.70 ± 0.7^{bcd}	2.279 ± 0.039^{i}
9	40.95 ± 0.8^{d}	45.38 ± 0.6^{d}	50.69 ± 1.2^{d}		76.70 ± 1.8^{a}	80.72 ± 0.5^{a}	85.31 ± 0.6^{abcd}	2.645 ± 0.045^{g}
12	54.43 ± 2.1^{c}	59.85 ± 0.3^{c}	64.06 ± 1.3^{c}		77.05 ± 0.8^{a}	81.08 ± 1.1^{a}	85.88 ± 0.8^{abcd}	2.942 ± 0.032^{e}
15	62.58 ± 0.9^{b}	68.42 ± 1.4^{b}	72.66 ± 0.2^{b}		77.34 ± 0.7^{a}	81.37 ± 0.8^{a}	86.28 ± 1.3^{abcd}	3.167 ± 0.016^{c}
16	69.82 ± 0.2^{a}	74.29 ± 1.2^{a}	79.93 ± 2.8^{a}	0.046 ± 0.003^{b}	77.61 ± 1.4^{a}	81.63 ± 0.4^{a}	86.64 ± 1.9^{abc}	3.286 ± 0.025^{b}
20 W/g								
2	− 14.07 ± 0.7^{g}	− 9.02 ± 0.4^{g}	− 3.48 ± 0.7^{g}		75.98 ± 0.2^{a}	80.13 ± 0.6^{a}	84.08 ± 0.1^{de}	1.807 ± 0.055^{j}
4	22.59 ± 1.8^{e}	27.48 ± 1.4^{e}	32.98 ± 0.5^{e}		76.49 ± 0.5^{a}	80.64 ± 1.2^{a}	85.27 ± 1.6^{abcd}	2.289 ± 0.019^{i}
6	41.34 ± 0.3^{d}	46.22 ± 1.2^{d}	51.93 ± 0.9^{d}		76.95 ± 1.4^{a}	81.10 ± 0.8^{a}	86.23 ± 0.3^{abcd}	2.767 ± 0.023^{f}
8	54.67 ± 2.3^{c}	60.32 ± 1.5^{c}	65.33 ± 2.1^{c}		77.36 ± 0.2^{a}	81.51 ± 0.7^{a}	87.04 ± 0.6^{ab}	3.114 ± 0.014^{c}
10	70.59 ± 0.8^{a}	75.73 ± 1.6^{a}	80.46 ± 1.5^{a}	0.018 ± 0.001^{c}	77.70 ± 0.4^{a}	81.85 ± 0.6^{a}	87.68 ± 0.7^{a}	3.389 ± 0.018^{a}

Data are shown as mean ± SD (n = 3). Different letters in the same column indicate significant difference at $p < 0.05$.

70.59 °C when treated at 10 W/g, 15 W/g and 20 W/g, respectively. This finding was consistent with the various reduced degree of the relative areas of cytoplasmic bulk water (A_{22}) according to different microwave power densities. ΔC_p at T_g is decreased by cross-linking with the increase of microwave power density and there are no detectable ΔC_p at T_g in some parts of Table 1. This result might be explained by the fact that cross-linking reduces the number of chains thermally activated and by the chain mobility, and thus raises the glass transition temperature and diminishes the change in specific heat capacity ΔC_p (Chung, Woo, & Lim, 2004).

The process of MVD caused a slight increase in T_0, T_P and T_c. With the increase of drying time, T_0, T_P and T_c of lotus seeds were shifted to higher temperatures. These temperatures increased at a larger extent with the increase of microwave power density. Zhong et al. (2013) also found that when compared with untreated samples, the gelatinization temperature of microwave irradiation-treated rice flour was shifted to higher temperatures. Meanwhile, ΔH of microwave irradiation-treated samples exhibited enthalpy levels 68.41–88.49% greater than the corresponding values for fresh samples (Table 1). The high gelatinization enthalpy indicated that more energy was required for the gelatinization of these starch granules. Two possible explanations exist as to why the enthalpy of gelatinization increases as samples are dried with a higher microwave power density. This could be explained by an annealing effect and the hydration of starch granules when the increase of microwave power density results in the samples being heated more rapidly (Bilbao-Sáinz, Butler, Weaver, & Bent, 2007). This was consistent not only with the decrease of the relaxation times of cytoplasmic bulk water (T_{22}) mentioned above, which results in enhancing the binding force between water and protein, but also with the increased amount of the relative areas of free water (A_{23}). Thus, the availability of water that could be used for starch hydration and swelling was limited and more energy was needed for gelatinization (Ding et al., 2015).

These observations indicate that the increase in the T_g and T_P of lotus seeds caused by applying MVD depends on the microwave power density. Hence, to improve the T_g and T_P of lotus seeds by MVD, an appropriate microwave power density should be carefully considered.

3.2.2. Water state as measured by NMR

TD-NMR spectrometry was applied by registering T_2 weighted relaxation curves to obtain a detailed view of the distribution of water inside the cellular structures of lotus seeds as a function of microwave power density. In fact, aside from water, other material could affect T_2. However, CPMG delay curves, which was used to measure T_2 collected from the poor signal of high molecular weight materials, such as starches, was caused by the relaxation time occurring too rapidly for the data to be collected. Thereby, the signal of starches could be neglected in terms of TD-NMR in this study. In terms of the small amount of low molecular weight sugars that came into being during MVD, their signals probably contributed to the relaxation times of bound water (T_{21}) and also contributed a small amount to the T_{22} populations; therefore, how they affected T_2 was not clear in this study and will be studied further in a future study. The intermediate amount of bound water (T_{21}) with the shortest relaxation time (0.01 ms < T_{21} < 10 ms) was ascribed to cell wall water. In addition, the largest population of cytoplasmic bulk water (T_{22}) with intermediate relaxation time (10 ms < T_{22} < 70 ms) and the small amount of free water (T_{23}) with the longest relaxation time (T_{23} < 70 ms) were assigned to cytoplasmic plus extracellular water and vacuolar water, respectively (Fig. 2). The T_{22} and T_{23} were the main population groups representing 97–99% of water present in lotus seeds and, T_{21} was negligible in the initial distribution. This has been commonly observed in fruits and vegetables, and also agrees with the results in carrots (Xu et al., 2014). Therefore, only these two main population groups were analyzed further Fig. 3.

Fig. 2 shows the distribution of T_2 relaxation times of samples affected by the various microwave power density treatments applied during MVD. As drying time increased, the samples undergoing MVD had a larger bonding force and their peak positions were shifted to the left side on the signal intensity-T_2 curve under all conditions studied here. This indicated that MVD at any of the tested strengths (10 W/g, 15 W/g or 20 W/g) could result in a decrease in water mobility with increasing drying time. A_{22} values, which represented the peak area of cytoplasmic bulk water among the three treatments all initially increased. This increase may be caused by the shift of free water to cytoplasmic bulk water result-

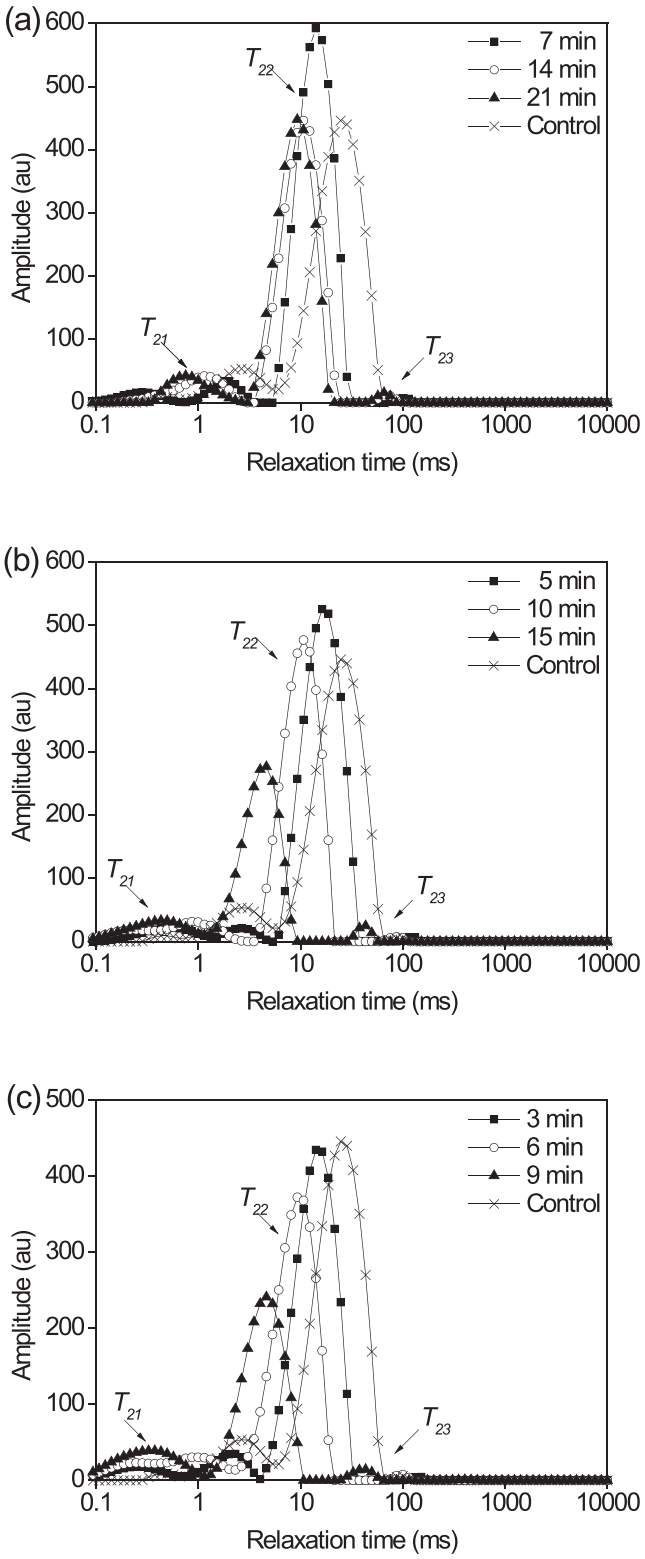


Fig. 2. Distribution of T_2 relaxation times of samples affected by the various microwave power density treatments applied during microwave vacuum drying: (a) 10 W/g; (b) 15 W/g; (c) 20 W/g.

ing from the increase in the concentration of carbohydrates (mainly glucose, fructose and sucrose) and the degradation of nutritional ingredients in the cytoplasm (Xin et al., 2013). Then, A_{22} decreased continuously with increasing drying time because of the shift of cytoplasmic bulk water to water more tightly bound to the polysaccharides in the cell wall. This might explain the increase in A_{21}, which represented the peak area of bound water.

T_{21} and T_{22} decreased and their peak positions were shifted to the left side on the signal intensity-T_2 curve with an increase in microwave power density. This observation was in accordance with decreases in T_{22} when microwave power increased (Xin et al., 2013). Han, Wang, Xu, and Zhou (2014) reported denaturation in reacting systems might explain the decrease of T_{21} and T_{22}. Furthermore, the results showed that A_{21} increased and A_{22} decreased as the microwave power density increased from 10 W/g to 20 W/g. The changes of A_{21} and A_{22} were larger at higher power density levels; this phenomenon might be caused by overly rapid heating under microwaves, resulting in the breaking of cell membranes.

3.2.3. Relationship between the T_g as well as T_P and water state in microwave vacuum dried lotus seeds

The results of the correlation analysis (Table 2) show that T_g was correlated negatively with the relaxation times of both T_{21} ($p < 0.05$) and T_{22} ($p < 0.01$) as well as the relative areas of A_{21} ($p < 0.05$), A_{22} ($p < 0.01$) and A_0 ($p < 0.05$) in lotus seeds. Xin et al. (2013) stated that the T_g of osmotically treated broccoli was correlated negatively with the relaxation times of the T_{21} and T_{22} and the relative areas of the A_{22}. In addition, a regression equation ($T_g = 3968.293–16.754A_{22}$ ($R^2 = 0.94$; $p < 0.01$)) and an equation from path analysis ($T_g = -0.968A_{22}$ ($R^2 = 0.94$; $p < 0.01$)) were obtained in the present study. These equations showed that the T_g had a linear relationship with A_{22} and that changes in the T_g were affected appreciably by A_{22}. Compared with the effects of cytoplasmic bulk water, the effects of bound water were not as appreciable ($p < 0.05$). In addition, compared with the correlation between the relaxation times and T_g, the correlation between the relative areas and T_g was higher. This finding may occur because the related areas directly reflect the relative content of water at different states. However, the T_2 observed was related to both the water and the mobility of the components, when theirs proton were exchanging during hydration (Xin et al., 2013). This study did not clearly show how the mobility of the components affect T_2 and this will be analyzed further a future study. Nevertheless, a significantly negative relationship was observed between A_{22} and T_g. The reason for the increased T_g may be the shift from cytoplasmic bulk water to bound water, which has a rapid proton chemical exchange effect with hydroxyl protons on the polysaccharides in the rigid cell wall (e.g., pectin). Pectin possesses three types of hydrophilic groups in its molecular structure that can reduce the dynamic mobility of the surrounding water and increase local viscosity (Einhorn-Stoll, Hatakeyama, & Hatakeyama, 2012). This observation was in accordance with the decrease in A_{22} and increase in A_{21}.

The T_P was correlated negatively with the relaxation times of T_{21} and T_{22} ($p < 0.01$) and the relative areas of A_{21}, A_{22} ($p < 0.05$) and A_0 ($p < 0.05$) in lotus seeds (Table 2). This indicated T_P might be affected by T_{21} and T_{22}, because the binding force increased when T_{21} and T_{22} decreased; this resulted in higher temperatures and more energy was needed for gelatinization.

3.3. Changes of PPO activity and color

The results of PPO activity determination at 10, 15 and 20 W/g showed that PPO did not exist after 4, 3 and 2 min during MVD, respectively (Fig. 3(a)). This occurs because PPO is very heat sensitive; the optimal reaction temperature of PPO in lotus seeds is about 45–50 °C (Chen, 2010), while during MVD, the temperature exceeds its reaction temperature in a few minutes (Fig. 3(b)). At the beginning of the MVD, oxygen in the cells could react with PPO until there was no oxygen and PPO left. Thus,

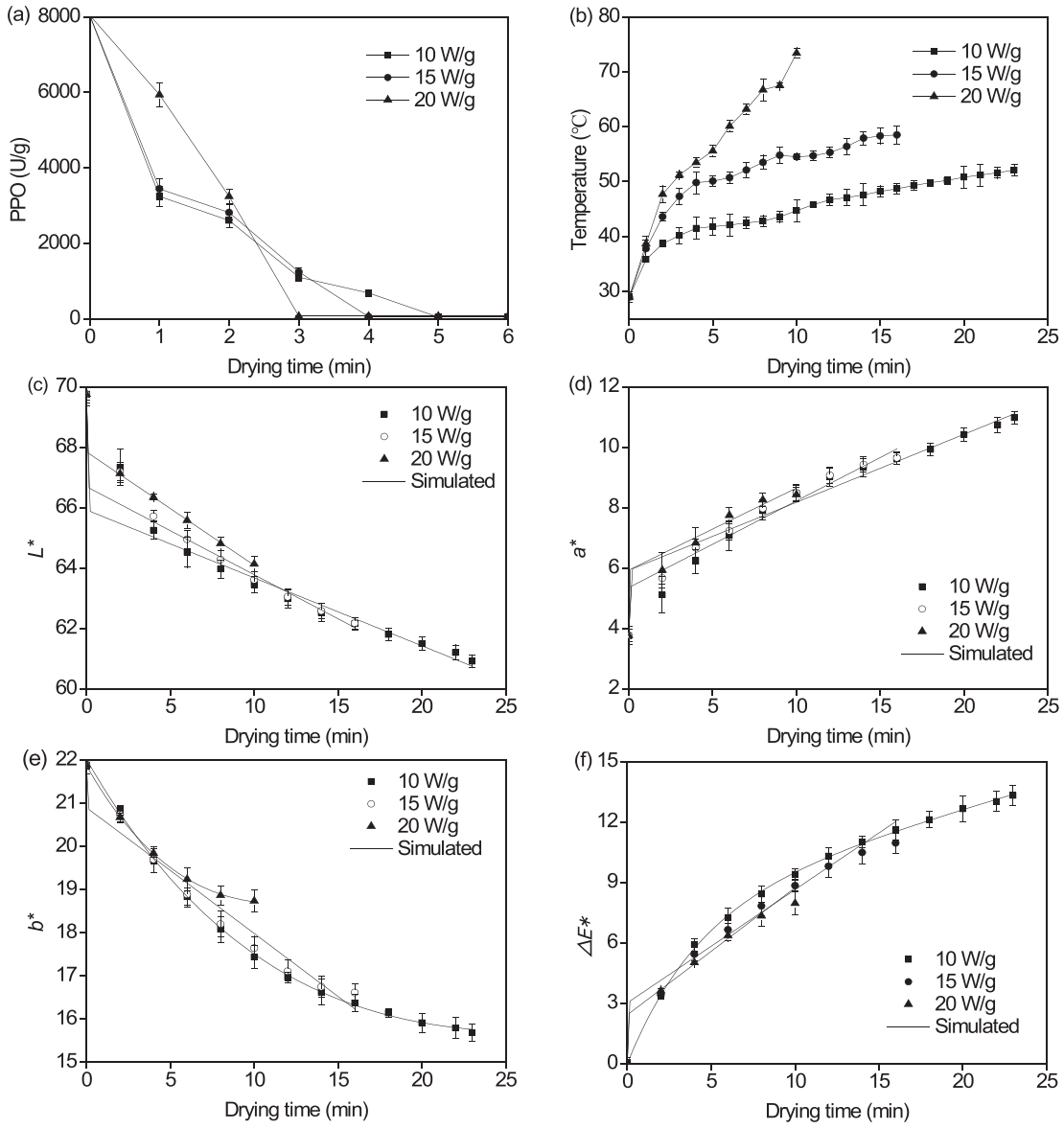


Fig. 3. Effect of different microwave power densities on (a) polyphenol oxidase activities; (b) surface temperature; (c) L^* values; (d) a^* values; (e) b^* values; (f) ΔE^* values of lotus seeds during microwave vacuum drying at 20 kPa of absolute pressure.

Table 2
Correlation coefficients between the water state and T_g as well as T_P in microwave vacuum dried lotus seeds.

Coefficient	T_{21}	A_{21}	T_{22}	A_{22}	A_0
T_g	−0.952*	−0.489*	−0.846**	−0.968**	−0.970*
T_P	−0.999**	−0.674	−0.972**	−0.987*	−0.987*

A_0, A_{21} and A_{22} are relative areas reflecting the relative content of total water, bound water and cytoplasmic bulk water, respectively.
* and ** indicate the correlation is significant at the $p < 0.05$ and 0.001 levels, respectively.

non-enzymatic browning was considered a major cause of color changes of dried lotus seeds in the subsequent MVD. The higher degree of non-enzymatic browning that occurred during MVD might be only caused by the Maillard reaction. This could be explained by the fact that there was no oxygen left in the drying chamber. Therefore, the main cause of non-enzymatic browning could be only the Maillard reaction (Pei et al., 2014). As a result, the rates of change of color were observed to be divided roughly into two periods, consisting of a rapid change caused by enzymatic browning and a slow change caused by non-enzymatic browning (Fig. 3(c)–(f)). The drying time that identified the end point of the period where the rates of change of color were rapidly changing was the same as the time that divided the drying curves into the first and second falling rate periods.

Values of color parameters for fresh lotus seeds were: $L^* = 69.76 \pm 0.16$, $a^* = 3.76 \pm 0.24$ and $b^* = 21.89 \pm 0.32$ (Fig. 3(c)–(e)). The change in the brightness of dried samples can be taken as a measurement of browning, which reduced from 69.76 to 60.90, 62.17 and 64.13 during MVD at microwave power densities of 10, 15 and 20 W/g, respectively. Meanwhile, it was found that

with an increase of drying time, there is an increase in a^* (124.20–191.75%) and a decrease in b^* (14.40–28.37%). The decrease in b^* may be caused by non-enzymatic Maillard browning, and formation of brown pigments (Dadali, Demirhan, & Özbek, 2007). Figiel (2009) also reported that garlic cloves are shifted to a little towards red and a bit more towards blue during MVD. Regarding the samples dried with the MVD, it was found that with an increase in microwave power density, an increase in L^* and b^*, and a decrease in a^* and ΔE occurred. However, the opposite trends were found in the color change reported by Dadali et al. (2007) who stated L^* and b^* decreased and a^* and ΔE increased when the power was increased in during microwave drying of spinach and okra. This different phenomenon might be caused by the effects of low pressure during microwave irradiation. Therefore, the comparison of the change of color during MVD and microwave drying would require further study. The change of L^* concurred with a report that stated the brightest color were whole garlic cloves dried at 720 W, and darkest were slices dried at 240 W (Figiel, 2009).

A new model was selected to predict the color kinetics of lotus seeds under MVD. The fitting procedure indicated that the results obtained from Eq. (4) could be used to model the color behavior of lotus seeds (Fig. 3(c)–(f)). Eq. (4) shows a close fit existed with the various experimental color data L^*, a^*, b^* and ΔE simultaneously and had a relatively high R^2 that ranged from 0.9759 to 0.9878, 0.9759 to 0.9878, 0.9759 to 0.9878 and 0.9759 to 0.9878 with L^*, a^*, b^* and ΔE, respectively.

3.4. Rehydration capacity

Fig. S2 shows that rehydration curves exhibited an increase in water content with time. The rehydration kinetics involve an initial high rate of water absorption followed by a slower rehydration rate in the end of rehydration. The high water gain during the beginning of rehydration is due to surface adsorption and capillary action (Seremet, Botez, Nistor, Andronoiu, & Mocanu, 2016). However, the decrease in the rehydration rate observed over time is related to the decrease of the driving force for water transfer as rehydration progresses and the system approaches equilibrium (Moreira et al., 2008). Furthermore, the rehydration time that demonstrated the rehydration curves had high and slow rehydration rate periods was the same as the time that divided the drying curves into the first and second falling rate periods. In addition, all conditions tested here showed the moisture content of microwave vacuum dried lotus seeds did not reach the initial moisture content before drying (1.65 g/g d.b.). This type of behavior was reported in a few similar studies regarding microwave dried spinach (Dadali et al., 2007). Moreira et al. (2008) proposed that leaching flows need to be considered when the water transfer during the rehydration process was evaluated. However, their results also indicated that the leaching flow is practically zero in samples pre-dried to high moisture content (values higher than 0.33 kg/kg d.b.). That is why this study neglected to analyze leaching flows.

The Peleg model was used to fit the experimental data in this study and the data were fitted very well ($R^2 > 0.9900$; Fig. S2). The estimated parameters, k_1 and k_2, of Peleg's model for a given condition are also given in Table 3. The values of the kinetic rate constant k_1 and characteristic constant k_2 were observed to decrease with an increase in microwave power density. These occurred because as the microwave power density increased, the rehydration and equilibrium moisture content increased, which was supported by the decrease in k_2 based on Eq. (7) between equilibrium moisture content and k_2. Water transfer (related to the inverse of k_1) is promoted by an increase in microwave power density and leads to a more rapid rehydration rate at higher microwave power densities (Dadali et al., 2007). The statistical values of k_1 and k_2 (using the standard error and coefficient of determination (R^2)) versus W_p accurately fit to Eqs. (8) and (9) were 0.4527×10^{-6}, ($R^2 = 0.999$) and 1.1205×10^{-6} ($R^2 = 0.999$). Then, k_0 and h_0 as well as A and B values were estimated as 1.8948 (s (g d.b./g)), 826.6834 (s (g d.b./g)) and 0.0136 g/W, 0.0844 g/W, respectively.

Table 3
Parameters and regression co-efficient of the different models applied to rehydration kinetics at different microwave power density treated lotus seed samples.

	10 W/g	15 W/g	20 W/g
k_1	355.425[a]	233.736[b]	152.563[c]
k_2	1.653[a]	1.542[b]	1.441[c]
R^2	0.995	0.996	0.997

Different letters in the same row indicate significant difference at $p < 0.05$.

3.5. Changes in chemical composition

Table S2 indicates that the change of main nutrients content including water, ash, fat, crude protein and carbohydrate in lotus seeds dried by microwave vacuum drying at different conditions. This result showed that only the contents of crude protein and carbohydrate were significantly different under various drying conditions. In fact, amino acid and starch were the main components of proteins and carbohydrates. Therefore, only amino acid and starch were shown in Tables S3–S4. Amino acids, as the main contributors to taste, are often lost, changed or even destroyed during drying depending on drying conditions. Table S3 displays the changes in the composition and quantity of free amino acids before and after drying under different drying situations. A total of 17 amino acids were identified in these samples out of which the average amounts of arginine (Arg), aspartic acid (Asp), and serine (Ser) were greater than 80 mg/100 g d.b. in fresh samples. They were the most abundant free amino acids found in lotus seeds samples; however, this result was inconsistent with the reports from Zeng, Cai, Cai, Wang, and Li (2013) and Wu et al. (2007) when glutamic acid (Glu) was reported to be the most abundant component of non-essential amino acids in lotus seed proteins and embryos, respectively. The content of total free amino acids in fresh samples was 490.81 mg/100 g d.b. and the amount of Asp constituted the highest level of non-essential amino acids (83.18–112.73 mg/100 g d.b.). MVD resulted in a significant ($p < 0.05$) improvement in the total free amino acid content compared with those in the fresh sample, reaching a maximum value of 540.19 mg/100 g d.b. when treated at 20 W/g (Table S3). These results were in agreement with the literature that high temperatures may promote proteolysis of amino acids during drying (Yoneda, Okubo, Kasai, & Hatae, 2005). A similar trend was observed for the total of both essential and non-essential amino acids (Table S3).

However, in terms of each individual amino acid, most content of non-essential amino acids in fresh lotus seeds increased while essential amino acids decreased when undergoing MVD. In addition, the products dried at higher microwave power density contained more total amino acids than those dried at lower ones, which could be attributed to the short drying time of MVD at 20 W/g (Fig. 1). Methionine (Met) is the primary limiting amino acid in lotus seeds (Guo, Xu, Chi, Jia, & Zeng, 2015). Met content showed a decreasing trend during MVD because it is labile to heating and the evaporation and/ degradation of more volatile compounds (Soria, Sanz, & Villamiel, 2008). However, it could be enhanced with MVD, because samples pretreated by MVD might tend to produce more peptides with a C-terminal hydrophobic amino acid residue than untreated samples. Irrespective of microwave power, Met content did not vary significantly among different microwave power densities. In addition to these findings, the degree of the Maillard reaction decreased with a reduced drying

time when using a higher microwave density. This was consistent with the higher L^* observed at 20 W/g. The Maillard reaction made the use of Glu and Asp (El-Hady & Albishri, 2015), which gave rise to a smaller loss of Glu and Asp and more of these two proteins was left with higher microwave density. However, further study will be needed to determine why the contents of Glu and Asp in dried lotus seeds were greater than that in fresh ones and how they can be biosynthesized during MVD will also be studied. Nonetheless, MVD can improve the content of free amino acids in lotus seed.

Table S3 also divided these free amino acids into several classes based on their taste characteristics, as suggested by Komata (1969). Asp and Glu are both monosodium glutamate-like (MSG-like) components of lotus seeds, and serve as the two major flavor-producing amino acids. The combined values for these two amino acids in dried samples ranged from 112.33 to 125.32 mg/100 g d.b. (Table S3), which was lower bitter components (201.32–213.04 mg/100 g d.b.) while higher than those of sweet (99.79–112.79 mg/100 g d.b.). However, MVD resulted in no significant difference ($p > 0.05$) in terms of the content of tasteless amino acid components of the samples. Our results suggest that the use of MVD could result in increased amounts of taste-active amino acids.

The Maillard reaction also involved reducing sugars, except for when the Maillard reaction involves amino acids. Considering starches were the major carbohydrates in lotus seeds, the changes of starches after various MVD are shown in Table S4. Generally, the content of total starches significantly ($p < 0.05$) decreased with MVD compared with fresh one. This phenomenon might be related to drying temperature, because Hódsági et al. (2012) reported that microwave heating resulted in an increase of starch content while a decreased starch content was found in samples treated with freeze drying (Pei et al., 2014). This reduction may also be caused by the Maillard reaction, which occurred during heat treatment. In addition, an increase in the microwave power density resulted in a decrease in the content of total starch. This was attributed to part of starch being altered into a form that was not easily hydrolyzed by enzymes or into macromolecular substances such as proteins; cellulose closely resembles starch and causes recombinations between enzymes and starches (Chen, 2015). A similar trend was seen in amylose. Amylose content decreased with increasing microwave power density, ranging from 6.97 to 6.52 g/100 g d.b. This occurred because long chain branching of amylopectin also complexed with iodine and amylose was changed into complex molecules during higher microwave power density treatment (Chen, 2015). The resistant starch type 3 content treated by higher microwave power density was lower than that by lower microwave power density. This might occur because the more rapid heating treatment caused by 20 W/g MVD during gelatinization and the amylose could not absolutely outflow from native starch, which reduced the formation and content of resistant starch type 3 (Zeng et al., 2015). The same decreased trend of the content of amylose and resistant starch confirmed the positive correlation between amylose and resistant starch which was also reported by Li, Jiang, Campbell, Blanco, and Jane (2008) in a previous study.

4. Conclusions

In this study, the effects of microwave power densities on drying characteristics of lotus seeds were investigated using a microwave vacuum dryer. The drying time of lotus seeds during MVD decreased by an average of 56.52% when using a relatively high microwave power density of 20 W/g compared with drying at 10 W/g. Two falling rate periods were observed during MVD. The drying kinetics involved an initial high rate of water removal followed by slower water removal in the end of the drying process. D_{eff} was calculated at 1.094×10^{-5} (m^2/s) at 20 W/g, which resulted in a significant improvement of the drying rate by 127.44%. From the combination of TD-NMR and DSC, the results showed that T_2 and A_2 were correlated negatively with T_g and T_P. MVD enhanced the T_g appreciably based on the decreased content of A_{22}. A new model proposed in this study has proven to be quite good at describing the color behavior of lotus seeds during MVD. To preserve the color, enzymatic and non-enzymatic browning should be reduced. Indeed, as demonstrated in this study, higher microwave power density could help reduce both enzymatic and non-enzymatic oxidative reactions. Moreover, the rehydration characteristics were correlated positively with increasing microwave power density because of the relationship between k_1 and k_2 of the Peleg's model with microwave power density. This study also showed that lotus seed dried with MVD at higher microwave power possessed a significantly higher content of total free amino acids (especially the taste-active amino acids) but had lower starch content because of the Maillard reaction.

Acknowledgements

The research was financially supported from projects of the National Natural Science Foundation of China (Grant No. 31401616), the Specialized Research Fund for the Doctoral Program of Higher Education (Grant No. 20133515120016), the Funds for Distinguished Young Scientists (Grant No. xjq201418), the Scientific and Technological Innovation Team Support Plan of Fujian Agriculture and Forestry University of China (Grant No. cxtd12009) and the High Level University Construction Project of Fujian Agriculture and Forestry University of China (Grant No. 612014042).

Appendix A. Supplementary data

Supplementary data associated with this article can be found, in the online version, at http://dx.doi.org/10.1016/j.foodchem.2017.01.141.

References

Aral, S., & Beşe, A. V. (2016). Convective drying of hawthorn fruit (*Crataegus* spp.): Effect of experimental parameters on drying kinetics, color, shrinkage, and rehydration capacity. *Food Chemistry, 210*, 577–584.

Bilbao-Sáinz, C., Butler, M., Weaver, T., & Bent, J. (2007). Wheat starch gelatinization under microwave irradiation and conduction heating. *Carbohydrate Polymers, 69*(2), 224–232.

Chen, B. Y. (2010). *Studies on the microwave vacuum drying of lotus-seed* MS thesis, Fujian Agriculture and Forestry University.

Chen, B. Y. (2015). *Effects of microwave irradiation on lotus seed starch* MS thesis, Fujian Agriculture and Forestry University.

Chung, H. J., Woo, K. S., & Lim, S. T. (2004). Glass transition and enthalpy relaxation of cross-linked corn starches. *Carbohydrate Polymers, 55*(1), 9–15.

Dadali, G., Demirhan, E., & Özbek, B. (2007). Color change kinetics of spinach undergoing microwave drying. *Drying Technology, 25*(10), 1713–1723.

Ding, X., Zhang, H., Wang, L., Qian, H., Qi, X., & Xiao, J. (2015). Effect of barley antifreeze protein on thermal properties and water state of dough during freezing and freeze-thaw cycles. *Food Hydrocolloids, 47*, 32–40.

Einhorn-Stoll, U., Hatakeyama, H., & Hatakeyama, T. (2012). Influence of pectin modification on water binding properties. *Food Hydrocolloids, 27*(2), 494–502.

El-Hady, D. A., & Albishri, H. M. (2015). Simultaneous determination of acrylamide, asparagine and glucose in food using short chain methyl imidazolium ionic liquid based ultrasonic assisted extraction coupled with analyte focusing by ionic liquid micelle collapse capillary electrophoresis. *Food Chemistry, 188*, 551–558.

Evin, D. (2012). Thin layer drying kinetics of *Gundelia tournefortii* L.. *Food and Bioproducts Processing, 90*(2), 323–332.

Figiel, A. (2009). Drying kinetics and quality of vacuum-microwave dehydrated garlic cloves and slices. *Journal of Food Engineering, 94*(1), 98–104.

Giri, S. K., & Prasad, S. (2007). Drying kinetics and rehydration characteristics of microwave-vacuum and convective hot-air dried mushrooms. *Journal of Food Engineering, 78*(2), 512–521.

Guo, Z. B., Xu, L. B., Chi, W. W., Jia, X. Z., & Zeng, S. (2015). Nutrient composition and in vitro glycemic index of lotus seeds harvested at different stages of maturation. *Current Topics in Nutraceuticals Research, 13*(4), 249.

Han, M., Wang, P., Xu, X., & Zhou, G. (2014). Low-field NMR study of heat-induced gelation of pork myofibrillar proteins and its relationship with microstructural characteristics. *Food Research International, 62*, 1175–1182.

Hódsági, M., Jámbor, A., Juhász, E., Gergely, S., Gelencsér, T., & Salgó, A. (2012). Effects of microwave heating on native and resistant starches. *Acta Alimentaria, 41*(2), 233–247.

Komata, Y. (1969). The taste and constituents of foods. *Nippon Shokuhin Kogyo Gakkaishi, 3*, 26.

Lewandowicz, G., Jankowski, T., & Fornal, J. (2000). Effect of microwave radiation on physico-chemical properties and structure of cereal starches. *Carbohydrate Polymers, 42*(2), 193–199.

Li, L., Jiang, H., Campbell, M., Blanco, M., & Jane, J. L. (2008). Characterization of maize amylose-extender (*ae*) mutant starches. Part I: Relationship between resistant starch contents and molecular structures. *Carbohydrate Polymers, 74*(3), 396–404.

Moreira, R., Chenlo, F., Chaguri, L., & Fernandes, C. (2008). Water absorption, texture, and color kinetics of air-dried chestnuts during rehydration. *Journal of Food Engineering, 86*(4), 584–594.

Nannyonga, S., Bakalis, S., Andrews, J., & Gkatzionis, K. (2016). Mathematical modelling of color, texture kinetics and sensory attributes characterisation of ripening bananas for waste critical point determination. *Journal of Food Engineering, 190*, 205–210.

Pei, F., Shi, Y., Gao, X., Wu, F., Mariga, A. M., Yang, W., ... Hu, Q. (2014). Changes in non-volatile taste components of button mushroom (*Agaricus bisporus*) during different stages of freeze drying and freeze drying combined with microwave vacuum drying. *Food Chemistry, 165*, 547–554.

Peleg, M. (1988). An empirical model for the description of moisture sorption curves. *Journal of Food Science, 53*(4), 1216–1217.

Ruiz-Cabrera, M. A., Rivera-Bautista, C., Grajales-Lagunes, A., González-García, R., & Schmidt, S. J. (2016). State diagrams for mixtures of low molecular weight carbohydrates. *Journal of Food Engineering, 171*, 185–193.

Ruiz-Cabrera, M. A., & Schmidt, S. J. (2015). Determination of glass transition temperatures during cooling and heating of low-moisture amorphous sugar mixtures. *Journal of Food Engineering, 146*, 36–43.

Schulze, B., Hubbermann, E. M., & Schwarz, K. (2014). Stability of quercetin derivatives in vacuum impregnated apple slices after drying (microwave vacuum drying, air drying, freeze drying) and storage. *LWT – Food Science and Technology, 57*(1), 426–433.

Seremet, L., Botez, E., Nistor, O.-V., Andronoiu, D. G., & Mocanu, G.-D. (2016). Effect of different drying methods on moisture ratio and rehydration of pumpkin slices. *Food Chemistry, 195*, 104–109.

Song, H., Zheng, B., & Zeng, S. (2009). *Stereo collocation microwave vacuum drying machine*. PR China: PRC Utility Model Patent Publication.

Soria, A. C., Sanz, J., & Villamiel, M. (2008). Analysis of volatiles in dehydrated carrot samples by solid-phase microextraction followed by GC–MS. *Journal of Separation Science, 31*(20), 3548–3555.

Tian, Y. T., Zhang, Y., Zeng, S. X., Zheng, Y. F., Chen, F., & Guo, Z. B. (2012). Optimization of microwave vacuum drying of lotus (*Nelumbo nucifera* Gaertn.) seeds by response surface methodology. *Food Science and Technology International, 18*(5), 477–488.

Wu, J. Z., Zheng, Y. B., Chen, T. Q., Yi, J., Qin, L. P., Rahman, K., & Lin, W. X. (2007). Evaluation of the quality of lotus seed of *Nelumbo nucifera* Gaertn from outer space mutation. *Food Chemistry, 105*(2), 540–547.

Xin, Y., Zhang, M., & Adhikari, B. (2013). Effect of trehalose and ultrasound-assisted osmotic dehydration on the state of water and glass transition temperature of broccoli (*Brassica oleracea* L. var. *botrytis* L.). *Journal of Food Engineering, 119*(3), 640–647.

Xu, C., Li, Y., & Yu, H. (2014). Effect of far-infrared drying on the water state and glass transition temperature in carrots. *Journal of Food Engineering, 136*, 42–47.

Yoneda, C., Okubo, K., Kasai, M., & Hatae, K. (2005). Extractive components of boiled-dried scallop adductor muscle and effect on the taste of soup after mixing with chicken leg meat. *Journal of the Science of Food and Agriculture, 85*, 809–816.

Zeng, H. Y., Cai, L. H., Cai, X. L., Wang, Y. J., & Li, Y. Q. (2013). Amino acid profiles and quality from lotus seed proteins. *Journal of the Science of Food and Agriculture, 93*(5), 1070–1075.

Zeng, S., Wu, X., Lin, S., Zeng, H., Lu, X., Zhang, Y., & Zheng, B. (2015). Structural characteristics and physicochemical properties of lotus seed resistant starch prepared by different methods. *Food Chemistry, 186*, 213–222.

Zhao, Y., Wang, W., Zheng, B., Miao, S., & Tian, Y. (2016). Mathematical modeling and influence of ultrasonic pretreatment on microwave vacuum drying kinetics of lotus (*Nelumbo nucifera* Gaertn.) seeds. *Drying Technology*, in press.

Zheng, B. D. (2004). *Studies and applications on the main quality of germplasm resources of Chinese lotus-seed (Nymphaeaceae Nelumbo* Adans*)* PhD thesis. Fujian Agriculture and Forestry University.

Zhong, Y., Tu, Z., Liu, C., Liu, W., Xu, X., Ai, Y., ... Wu, J. (2013). Effect of microwave irradiation on composition, structure and properties of rice (*Oryza sativa* L.) with different milling degrees. *Journal of Cereal Science, 58*(2), 228–233.

Zielinska, M., & Markowski, M. (2016). The influence of microwave-assisted drying techniques on the rehydration behavior of blueberries (*Vaccinium corymbosum* L.). *Food Chemistry, 196*, 1188–1196.

Zielinska, M., & Michalska, A. (2016). Microwave-assisted drying of blueberry (*Vaccinium corymbosum* L.) fruits: Drying kinetics, polyphenols, anthocyanins, antioxidant capacity, colour and texture. *Food Chemistry, 212*, 671–680.